Circulation
Cardiovascular Interventions
JOURNAL OF THE AMERICAN HEART ASSOCIATION
American Heart Association
Learn and Live

Changes in Left Main Bifurcation Geometry After a Single-Stent Crossover Technique : An Intravascular Ultrasound Study Using Direct Imaging of Both the Left Anterior Descending and the Left Circumflex Coronary Arteries Before and After Intervention

Soo-Jin Kang, Gary S. Mintz, Won-Jang Kim, Jong-Young Lee, Jun-Hyok Oh, Duk-Woo Park, Seung-Whan Lee, Young-Hak Kim, Cheol Whan Lee, Seong-Wook Park and Seung-Jung Park

Circ Cardiovasc Interv 2011;4;355-361; originally published online June 28, 2011;
DOI: 10.1161/CIRCINTERVENTIONS.110.961045
Circulation: Cardiovascular Interventions is published by the American Heart Association. 7272 Greenville Avenue, Dallas, TX 72514
 Print ISSN: 1941-7640. Online ISSN: 1941-7632

Changes in Left Main Bifurcation Geometry After a Single-Stent Crossover Technique

An Intravascular Ultrasound Study Using Direct Imaging of Both the Left Anterior Descending and the Left Circumflex Coronary Arteries Before and After Intervention

Soo-Jin Kang, MD, PhD; Gary S. Mintz, MD; Won-Jang Kim, MD; Jong-Young Lee, MD; Jun-Hyok Oh, MD; Duk-Woo Park, MD, PhD; Seung-Whan Lee, MD, PhD; Young-Hak Kim, MD, PhD; Cheol Whan Lee, MD, PhD; Seong-Wook Park, MD, PhD; Seung-Jung Park, MD, PhD

Background—We assessed geometric changes responsible for acute lumen loss at the left circumflex coronary artery (LCX) ostium after crossover stenting from the left anterior descending coronary artery (LAD) to the left main artery.

Methods and Results—Twenty-three left main artery bifurcation lesions with a preprocedural angiographic diameter stenosis <50% at the LCX ostium were evaluated using prestenting and poststenting intravascular ultrasound pullbacks from both the LAD and the LCX. At the minimal lumen area (MLA) sites within the LCX ostium and at the LCX carina, the lumen, stent, plaque+media (P+M), and external elastic membrane (EEM) areas were measured; the EEM eccentricity was calculated at the LCX carina. The change in MLA within the LCX ostium (ΔL), the change in EEM area at the MLA site (ΔV), and the change in P+M area at the MLA site (ΔP) were calculated. The MLA within the LCX ostium significantly decreased from 5.4 mm^2 (first and third quartiles, 4.3 mm^2, 7.2 mm^2) prestenting to 4.0 mm^2 (3.0 mm^2, 4.8 mm^2) poststenting ($P<0.001$). The percent change in MLA within the LCX ostium correlated with changes in EEM eccentricity ($r=-0.414$, $P=0.049$) and percent change in EEM area at the MLA site ($r=0.626$, $P=0.001$). A smaller distal carina angle between the LAD and the LCX before stenting was associated with a greater percent reduction in lumen ($r=0.472$, $P=0.023$) and EEM ($r=0.402$, $P=0.048$) after stenting. In 18 lesions with >10% reduction of MLA within the LCX ostium despite the lack of direct relationship between ΔL and ΔP at the MLA site, ΔP closely correlated with the ratio of ΔV to ΔL ($r=-0.953$, $P<0.001$), suggesting that an increase in plaque at the LCX ostium contributed to the MLA loss relative to the decrease in EEM area.

Conclusions—Lumen loss at the LCX ostium frequently occurred after crossover stenting from the distal LM to the LAD. The main mechanism was carina shift that was associated with a narrow angle between the LAD and LCX. **(*Circ Cardiovasc Interv*. 2011;4:355-361.)**

Key Words: ultrasonography ■ coronary arteriosclerosis ■ stents

Although drug-eluting stent implantation for unprotected left main coronary artery (LM) stenosis is evolving into a feasible therapeutic alternative to bypass surgery, stenting lesions at the distal LM bifurcation location remains a challenge and a major determinant of adverse outcomes whether using a 1-stent or 2-stent approach.[1–3] In particular, when using a 1-stent crossover technique, there are 2 suggested mechanisms of acute luminal loss at the ostium of the left circumflex-carina shift versus plaque shift.[4–7] Intravascular ultrasound (IVUS) provides unique insights into the extent and distribution of coronary atherosclerosis preintervention and has been used to assess mechanisms and complications of stent implantation. The aims of the current IVUS study were to use present and poststent implantation IVUS imaging of both the left anterior descending coronary artery (LAD) and the left circumflex coronary artery (LCX) to assess and predict the geometric changes that are responsible for acute lumen loss at the LCX ostium after implanting a stent from the LAD to the LM (ie, the single-stent crossover technique) to treat a distal LM bifurcation stenosis.

Clinical Perspective on p 361

Methods

Subjects

Between June 2009 and June 2010, 97 patients who had a preprocedural angiographic diameter stenosis (DS) >50% of the distal LM

Received November 30, 2010; accepted April 18, 2011.

From the Department of Cardiology, University of Ulsan College of Medicine, Asan Medical Center, Seoul, Korea (S.-J.K., W.-J.K., J.-Y.L., J.-H.O., D.-W.P., S.-W.L., Y.-H.K., C.W.L., S.-W.P., S.-J.P.), and Cardiovascular Research Foundation, New York, NY (G.S.M.).

Correspondence to Seung-Jung Park, MD, PhD, Asan Medical Center, 388-1 Poongnap-dong, Songpa-gu, Seoul, South Korea 138-736. E-mail sjpark@amc.seoul.kr

Circ Cardiovasc Interv **is available at http://circinterventions.ahajournals.org** **DOI: 10.1161/CIRCINTERVENTIONS.110.961045**

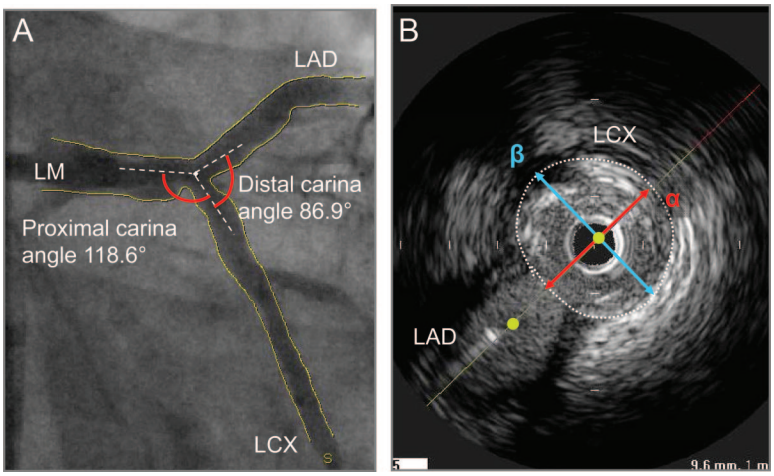

Figure 1. A, Quantitative coronary angiographic measurements of proximal and distal carina angles. **B**, Intravascular ultrasound measurement of external elastic membrane (EEM) eccentricity. Using an intravascular ultrasound frame of the LCX carina, α was defined as EEM diameter along the axis through the centers of both LAD and LCX lumens, and β was defined as EEM diameter perpendicular to the axis of α. EEM eccentricity index was calculated as β/α. LAD indicates left anterior descending coronary artery; LCX, left circumflex coronary artery; LM, left main artery.

and underwent percutaneous coronary intervention with a single-stent crossover technique from the LAD to the LM were prospectively enrolled. IVUS imaging of LAD and LCX both preprocedure and poststenting (immediately after crossover stenting from the LAD to the LM) was successfully performed in 33 patients. We excluded visible thrombus-containing lesions, the lesions with predilation of LCX before preprocedural IVUS, and LCX balloon inflations at any time before poststenting LCX pullback IVUS. Finally, 23 lesions in

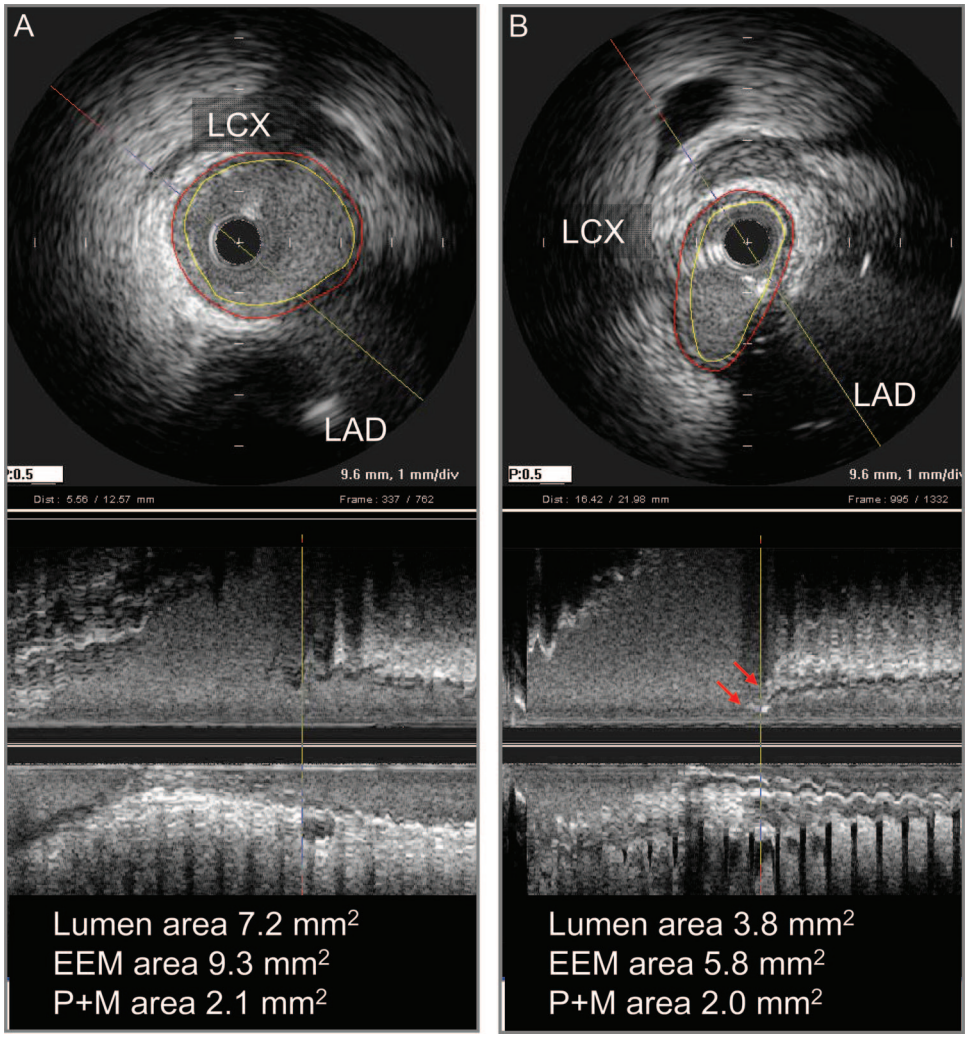

Figure 2. The LCX pullback intravascular ultrasound prestenting (**A**) and poststenting (**B**). After crossover stenting from LAD to LM, percent change in EEM area (red) was −38%, and percent change in lumen area (yellow) was −47%. However, the change in P+M area was not remarkable (2.08 mm^2 prestenting to 2.03 mm^2 poststenting). The longitudinal image reconstruction demonstrated carina shift into the LCX poststenting (arrows). EEM indicates external elastic membrane; LAD, left anterior descending coronary artery; LCX, left circumflex coronary artery; LM, left main artery; P+M, plaque plus media.

23 patients were analyzed. We obtained written informed consent from all patients, and the ethics committee approved this study.

Angiographic Analysis

Qualitative and quantitative angiographic analysis was done by standard techniques with automated edge-detection algorithms (CASS-5; Pie Medical Imaging; Maastricht, The Netherlands) in the angiographic analysis center of the CardioVascular Research Foundation, Seoul, Korea.[8–10] The Medina classification was used to describe the location and distribution of lesions at the LM bifurcation.[11] The angle between the proximal LM and the LCX (proximal carina angle) and the angle between the LAD and the LCX (distal carina angle) were measured before and after stenting (Figure 1A). The measurement was performed in the angiographic view in which the foreshortening of the 3 segments was minimal.[7,12–14]

IVUS Imaging and Analysis

IVUS imaging was performed after intracoronary administration of nitroglycerin 0.2 mg using motorized transducer pullback (0.5 mm/s) and a commercial scanner (Boston Scientific/SCIMED; Minneapolis, MN) consisting of a rotating 40-MHz transducer within a 3.2-F imaging sheath. Although a wire in the LCX was kept in place during stent deployment in the LAD at the operator's discretion, the jailed wire in the LCX was removed before LCX pullback IVUS. Using computerized planimetry (EchoPlaque 3.0; Indec Systems; MountainView, CA), offline IVUS analysis was performed in the IVUS core laboratory of Asan Medical Center (Seoul, Korea).

The carina was identified as the frame immediately distal to the take-off of the side branch.[15] Four segments of the LM bifurcation preintervention were defined using LAD pullback and LCX pullback. From the LAD pullback, the following were identified: (1) ostial LAD (3 mm distal to the carina), (2) polygon of confluence (confluence zone of LAD and LCX on longitudinal IVUS image reconstruction in parallel with the quantitative coronary angiography-based definition suggested by Ramcharitar et al[12] and modified for IVUS analysis[16]), and (3) distal LM (3 mm just proximal to the polygon of confluence). Separate from the LCX pullback, the ostium of the LCX (3 mm distal to the carina) was defined. At the minimal lumen area (MLA) site within each of these 4 segments, the lumen, stent, plaque plus media (P+M), and external elastic membrane (EEM) areas were measured by 2D planimetry. Plaque burden was calculated as P+M/EEM×100 (%). At the LCX carina, α was defined as the EEM diameter along the axis through the centers of both the LAD and the LCX lumens, and β was defined as the EEM diameter perpendicular to α. EEM eccentricity index was calculated as β/α (Figure 1B). Poststenting these 4 segments was identified in parallel with the preprocedural IVUS analysis, and both the minimal stent area within each segment and the stent, lumen, and EEM areas at the LCX ostium and carina were measured (Figure 2).[16]

Statistical Analysis

All statistical analyses were performed using SPSS version 10.0 (SPSS Inc; Chicago, IL) software. All values are expressed as the median value (first and third quartiles) for continuous variables or as counts and percentages for categorical variables. Continuous variables were compared by use of the nonparametric Mann-Whitney test, and Wilcoxon signed rank test was used to compare prestenting and poststenting continuous variables. Spearman rank correlation method was applied to estimate correlations between continuous variables. $P<0.05$ was considered statistically significant.

Results

The baseline clinical and procedural characteristics are summarized in Table 1. The angiographic data are shown in Table 2. All lesions had a preprocedural angiographic %DS <50% at the LCX ostium. The median acute change (prestent versus poststent implantation) in %DS of the LCX ostium was 11.7% (−3.2% to 18.0%). The Medina classifications were 1,1,0 in 65%, 1,1,1 in 18%, 1,0,0 in 9%, and 0,1,0 in 8%. All lesions had thrombolysis in myocardial infarction grade 3 flow at the LCX ostium before and immediately after stent implantation. There were no angiographic dissections at the LCX ostium during the procedure.

Table 1. Baseline Clinical and Procedural Characteristics

Variable	Value
Age, y	67.0 (56.0–71.0)
Male sex	16 (70)
Smoking	14 (60)
Hypertension	16 (70)
Hypercholesterolemia	15 (65)
Diabetes mellitus	11 (48)
Left ventricular ejection fraction	60.0 (55.8–62.0)
Previous myocardial infarction	2 (9)
Clinical presentation	
Stable angina	16 (70)
Unstable angina	6 (26)
Acute myocardial infarction	1 (4)
Types of drug-eluting stent	
Cypher	7 (31)
Xience	14 (61)
Endeavor-Resolute	1 (4)
Nobori	1 (4)
Total stent length, mm	46.0 (28.0–68.0)
Maximal balloon pressure, atm	20.0 (18.0–24.0)
Maximal balloon size, mm	4.3 (4.2–4.5)

Data are presented as median (interquartile range) or n (%).

Prestenting Versus Poststenting Angiographic and IVUS Findings

Overall, 19 (83%) of LCX ostia had an MLA ≥4.0 mm^2 preintervention, and 11 (48%) had an MLA <4.0 mm^2 poststenting. The median values of change in MLA within the LCX ostium and change in LCX carina area were −1.4 mm^2 (−2.0 mm^2, −0.6 mm^2) and −1.6 mm^2 (−2.7 mm^2, −0.9 mm^2), respectively.

Table 2. Angiographic Data in 23 LM Bifurcation Lesions Before Stenting

Variable	Value
Preprocedural	
MLD within LM, mm	1.9 (1.5–2.3)
DS of LM, %	51.9 (44.1–58.3)
MLD within LAD ostium, mm	1.5 (1.2–1.8)
DS of LAD ostium, %	56.7 (45.6–64.9)
MLD within LCX ostium, mm	2.6 (2.3–2.8)
DS of LCX ostium, %	21.8 (12.6–37.9)
Proximal carina angle, °	111.9 (83.5–125.4)
Distal carina angle, °	83.9 (49.7–105.7)

Data are presented as median (interquartile range). DS indicates diameter stenosis; LAD, left anterior descending coronary artery; LCX, left circumflex coronary artery; LM, left main artery; MLA, minimal lumen area; MLD, minimal lumen diameter.

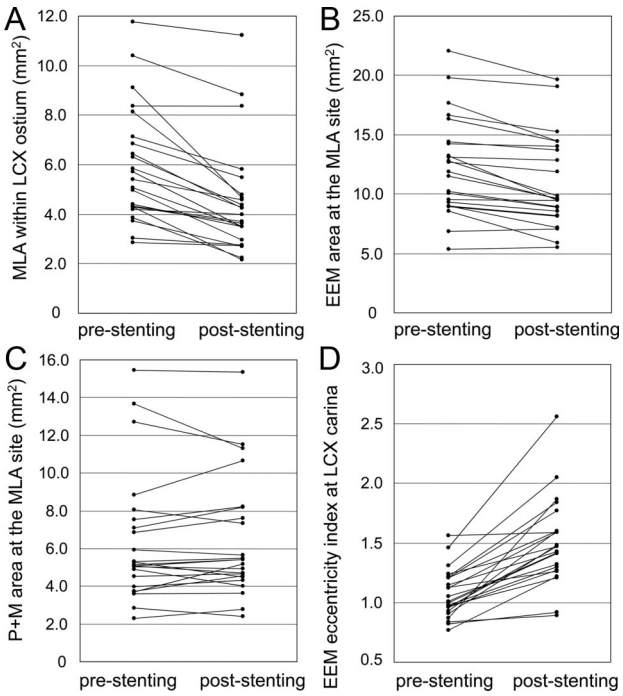

Figure 3. Prestenting and poststenting intravascular ultrasound parameters at the LCX ostium: MLA within the LCX ostium (**A**), EEM area at the MLA within the LCX ostium (**B**), P+M area at the MLA site within the LCX ostium (**C**), and eccentricity index at the LCX carina (**D**). EEM indicates external elastic membrane; LCX, left circumflex coronary artery; MLA, minimal lumen area; P+M, plaque plus media.

Preprocedural IVUS MLA did not correlated with the angiographic %DS at the LAD ostium ($r=-0.332$, $P=0.122$), at the LCX ostium ($r=-0.161$, $P=0.463$), or at the distal LM ($r=-0.202$, $P=0.356$). Moreover, the percent change in MLA at the LCX ostium from preintervention to poststent implantation showed no relationship with the change in angiographic %DS ($r=-0.206$, $P=0.347$).

Mechanisms of Luminal Loss of the LCX Ostium

Figure 3 demonstrated the changes in IVUS parameter of ostial LCX geometry during crossover stenting. The MLA within the LCX ostium significantly decreased from 5.4 mm^2 (4.3 mm^2, 7.2 mm^2) prestenting to 4.0 mm^2 (3.0 mm^2, 4.8 mm^2) poststenting ($P<0.001$) (Table 3). The lumen area at the LCX carina also decreased from 6.3 mm^2 (4.9 mm^2, 8.4 mm^2) prestenting to 4.3 mm^2 (3.4 mm^2, 5.8 mm^2) poststenting ($P<0.001$). Finally, the LCX became more eccentric as evidenced by an increase in EEM eccentricity index from 1.22 (0.97, 1.47) prestenting to 1.47 (1.27, 1.6) poststenting ($P=0.004$). Conversely, in the overall group of 23 patients, P+M area did not change at the LCX carina (5.2 mm^2 [3.7 mm^2, 8.7 mm^2] prestenting to 5.4 mm^2 [4.4 mm^2, 8.2 mm^2] poststenting, $P=0.323$) or at the MLA site within the LCX ostium (5.2 mm^2 [4.0 mm^2, 7.5 mm^2] prestenting to 5.4 mm^2 [4.5 mm^2, 8.2 mm^2] poststenting, $P=0.670$).

The percent change in MLA within the LCX ostium and the percent change in LCX carina area were −20.2% (−38.7%, −14.3%) and −30.9% (−40.2%, −15.0%), respectively. The percent change in MLA within the LCX ostium significantly correlated with the changes in EEM eccentricity index ($r=-0.414$, $P=0.049$) (Figure 4) and percent change in EEM area at the MLA site ($r=0.626$, $P=0.001$). Similarly, the percent change in lumen area at the LCX carina correlated with changes in EEM eccentricity index ($r=-0.388$, $P=0.050$) and percent change in EEM area at the LCX carina ($r=0.680$, $P<0.001$).

A reduction of MLA within the LCX ostium >10% was observed in 18 (78%) lesions, all of which had a decrease in EEM area. The change in MLA within the LCX ostium (ΔL) positively correlated with the change in EEM area at the MLA site (ΔV) ($r=0.670$, $P=0.002$) (Figure 5) and negatively correlated with the change in EEM eccentricity index at the LCX carina ($r=-0.591$, $P=0.010$). Despite the lack of direct relationship between ΔL and the change in P+M area at the MLA site (ΔP) ($r=-0.099$, $P=0.696$), ΔP closely correlated with $\Delta V/\Delta L$ ($r=-0.953$, $P<0.001$), suggesting that an increase in plaque at the LCX ostium contributed to

Table 3. Prestenting and Poststenting Intravascular Ultrasound Findings

	Prestenting	Poststenting
At the LAD ostium		
Lumen area at the MLA site, mm^2	4.0 (2.8–5.2)	
EEM area at the MLA site, mm^2	13.2 (10.8–14.7)	
Plaque burden at the MLA site, %	68.2 (60.9–79.2)	
Lumen area at carina, mm^2	4.7 (2.9–6.7)	
EEM area at carina, mm^2	14.0 (10.8–16.5)	
Plaque burden at carina, %	62.9 (58.5–76.7)	
MLA within the polygon of confluence, mm^2	6.0 (4.5–7.0)	
At the MLA site within distal LM		
Lumen area, mm^2	5.3 (3.5–8.0)	
EEM area, mm^2	17.9 (15.1–23.0)	
Plaque burden, %	68.5 (56.6–74.8)	
At the LCX ostium		
Lumen area at the MLA site, mm^2	5.4 (4.3–7.2)	4.0 (2.9–4.8)*
EEM area at the MLA site, mm^2	11.8 (9.0–14.4)	9.6 (8.2–14.0)*
Plaque burden at the MLA site, %	50.7 (38.3–58.6)	57.6 (50.0–62.4)*
Lumen area at carina, mm^2	6.3 (4.8–8.4)	4.3 (3.4–5.8)*
EEM area at carina, mm^2	12.8 (10.0–17.1)	9.7 (8.6–14.4)*
Plaque burden at carina, %	48.1 (36.7–54.5)	57.3 (49.4–60.7)*
Poststenting MSA within LAD ostium, mm^2		9.8 (8.1–10.3)
Poststenting MSA at LAD carina, mm^2		10.2 (9.3–10.8)
Poststenting MSA within the polygon of confluence, mm^2		11.0 (9.7–11.9)
Poststenting MSA within distal LM, mm^2		10.1 (11.1–12.4)

Data are presented as median (interquartile range). EEM indicates external elastic membrane; LAD, left anterior descending coronary artery; LCX, left circumflex coronary artery; LM, left main artery; MLA, minimal lumen area; MSA, minimal stent area.

*$P<0.001$ vs prestenting.

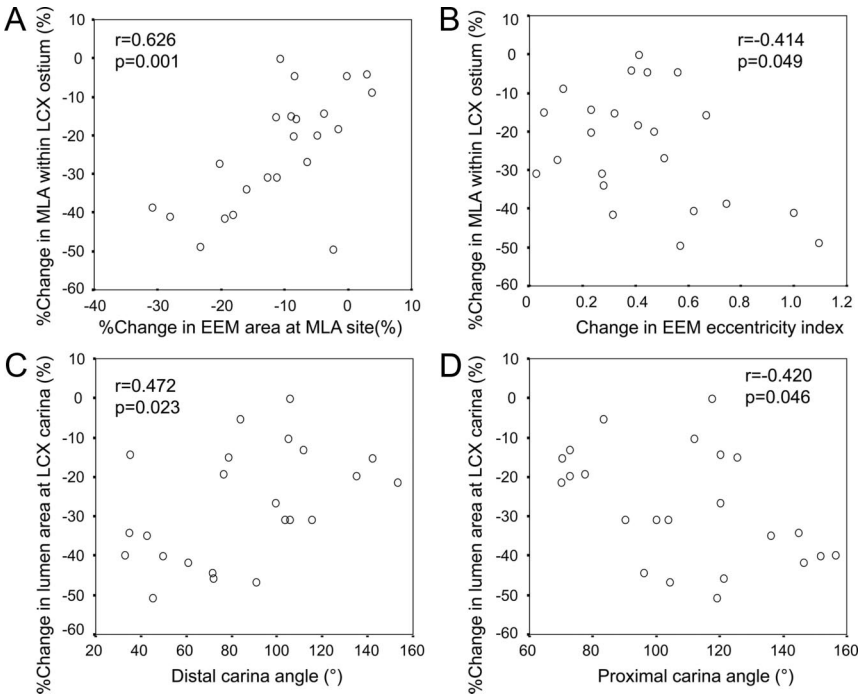

Figure 4. The percent change in MLA within the LCX ostium correlated with percent change in EEM area at the MLA site (**A**) and with the change in EEM eccentricity index (**B**). The percent change in lumen area at the LCX carina was related to the carina angle (**C** and **D**). Spearman rank correlation method was used to estimate correlations. EEM indicates external elastic membrane; MLA, minimal lumen area; LCX, left circumflex coronary artery.

the MLA loss relative to the decrease in EEM area. All 10 lesions with $\Delta V/\Delta L < 1$ showed $\Delta P > 0$. These 10 lesions had a greater ΔP (+0.73 mm^2 [0.23 mm^2, 1.18 mm^2] versus −0.40 mm^2 [−0.77 mm^2, −0.16 mm^2], $P<0.001$) and a greater increase in plaque burden (+10.22% [7.31%, 14.39%] versus +5.69% [3.02%, 8.60%], $P=0.037$) compared with the remaining 8 lesions with $\Delta V/\Delta L \geq 1$. There was no relationship between ΔP and the change in EEM eccentricity index ($r=0.333$, $P=0.347$).

Correlates of Luminal Loss at the LCX Ostium

Both a smaller distal angiographic carina angle prestenting ($r=0.472$, $P=0.023$) and a larger proximal angiographic carina angle prestenting ($r=-0.420$, $P=0.046$) were associated with a much greater percent reduction in lumen area of the LCX carina poststenting. Additionally, the distal carina angle prestenting ($r=0.402$, $P=0.048$) was related to the percent reduction in EEM area at the LCX carina poststenting. However, neither maximal balloon size ($r=0.154$, $P=0.4$) nor prestenting MLA within the LCX ostium ($r=0.046$, $P=0.8$) were related to the change in MLA within the LCX ostium. In addition, the change in MLA was not related to the preprocedural MLA within the LCX ostium ($r=0.042$, $P=0.8$), EEM area ($r=0.065$, $P=0.8$), or P+M area ($r=0.040$, $P=0.7$).

Treatment and Clinical Follow-Up

There were 10 (43%) lesions treated with kissing balloon inflations without stent implantation at the LCX. Clinical follow-up was performed in all patients at 12.8±5.1 months. One patient underwent target lesion revascularization because

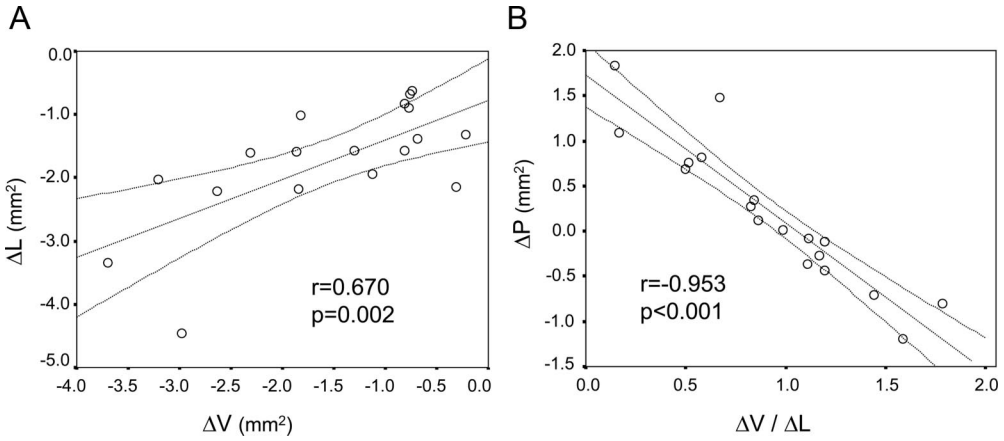

Figure 5. A, The relationship between the change in MLA within the LCX ostium (ΔL) and the change in EEM area (ΔV) in 18 patients in whom the percent reduction in MLA was >10%. **B**, The change in P+M area (ΔP) correlated with ΔV/ΔL in these lesions. Spearman rank correlation method was used to estimate correlations. EEM indicates external elastic membrane; MLA, minimal lumen area; LCX, left circumflex coronary artery; P+M, plaque plus media.

of restenosis of the LCX, and there was no death or myocardial infarction during the follow-up period.

Discussion

The major findings of this study are as follows: (1) Although most distal LM bifurcation lesions had only a mild stenosis of the LCX ostium prestenting, 78% showed a >10% reduction of MLA within the LCX ostium after crossover stenting from the LAD to the LM; (2) carina shift was the primary mechanism of ostial LCX lumen loss, and plaque redistribution was present but in fewer than half the lesions with a >10% reduction of MLA within the LCX ostium; and (3) narrow carina angle between the LAD and the LCX and wide carina angle between the LCX and the LM were associated with a greater lumen area loss at the LCX carina. A decrease in EEM area with EEM geometric change in most cases represented that the main mechanism of lumen area loss at the LCX ostium was carina shift during crossover stenting. Nevertheless, in the subgroup of lesions with $\Delta V/\Delta L < 1$ (fewer than half the lesions with a >10% reduction in MLA at the LCX ostium), plaque redistribution also contributed to lumen area loss.

Even though several studies reported the concept of carina displacement as the main mechanism of side branch compromise, few data demonstrate the geometric changes in LCX ostium by comparing prestenting and poststenting LCX pullback IVUS.[4–7] Previous studies used angiographic %DS to quantify the severity of LCX ostial stenosis. However, we found that the preprocedural angiographic %DS did not correlate with the IVUS MLA at the LCX ostium. Moreover, percent change in MLA at the LCX ostium did not correlate with the change in angiographic %DS. Furthermore, Oviedo et al[17] showed that the LCX ostium cannot be assessed tangentially from LAD to LM on IVUS pullback. Thus, the assessment of LCX ostium by direct LCX pullback is necessary to accurately evaluate LCX ostial stenosis in LM bifurcation lesions and the mechanisms of lumen loss during stent implantation.

The current study clearly demonstrated the morphological changes in LCX ostium using both LCX and LAD pullbacks before and after crossover stenting. Although preprocedural LCX ostial stenosis was not significant in most of these lesions, half showed a poststenting MLA within the LCX ostium <4.0 mm^2, with a significant decrease in measured MLA as the result of crossover stenting.

Because all lesions with a >10% reduction of MLA within the LCX ostium had a decrease in EEM area, carina shift (reduction in EEM associated with a more eccentric EEM shape) was the general mechanism of lumen loss at the LCX ostium during crossover stenting. In addition, because of the linear correlation between $\Delta V/\Delta L$ and ΔP, in a minority of lesions, plaque redistribution was superimposed on the geometric changes in size and shape of the EEM to contribute to LCX ostial lumen loss.

Gil et al[4] reported that a smaller distal carina angle predicted higher side branch compromise and major cardiovascular events at 1-year follow-up in patients with bifurcation lesions treated with a single main-vessel stent (crossover technique). The current data were consistent and extended these observations in that a smaller distal angiographic carina angle prestenting was associated with a much greater percent reduction in lumen area of the LCX carina poststenting because a smaller distal carina angle was a predictor of carinal shift, the main mechanism of lumen loss during crossover stenting.

Limitations

First, the current study evaluated selected lesions with normal or only mild stenosis at the LCX ostium prestenting. Although side branch pullback IVUS is essential, prestenting and poststenting assessment of the LCX ostium by direct LCX pullback was limited in many real-world cases because of the technical difficulty in passing the guidewire and then the IVUS catheter into the side branch through the tight lesions (before percutaneous coronary intervention) or stent struts (after percutaneous coronary intervention), especially when the turn into the LCX stenosis is tight. Nevertheless, if LCX pullback is successfully performed, it will provide useful information for the true severity of LCX ostial stenosis and the mechanism of LCX area change, particularly in the cases with side branch compromise after stenting. Second, physiological assessment of the LCX using fractional flow reserve was not performed. Therefore, we could not confirm the relationship between anatomic change of the LCX ostium and functional significance. Third, because of the lack of the follow-up data, the current study did not address the relationship of these IVUS findings to long-term clinical outcomes. Finally, the carina angle was obtained by quantitative coronary angiographic measurement. Even though the values were determined using multiple angiographic views after averaging several measurements, the 3D reconstruction by other modalities may be more accurate.

Conclusions

Lumen loss of the LCX ostium frequently occurs after crossover stenting for distal LM bifurcation lesions. Carina shift may be a main mechanism of lumen loss within the LCX ostium and was associated with a narrow distal angle between the LAD and the LCX and a wide proximal angle between the LCX and the LM. In a minority of patients, plaque redistribution may be superimposed on carinal shift to contribute to LCX ostial lumen area loss.

Disclosures

None.

References

1. Valgimigli M, Malagutti P, Rodriguez-Granillo GA, Garcia-Garcia HM, Polad J, Tsuchida K, Regar E, Van der Giessen WJ, de Jaegere P, De Feyter P, Serruys PW. Distal left main coronary disease is a major predictor of outcome in patients undergoing percutaneous intervention in the drug-eluting stent era: an integrated clinical and angiographic analysis based on the Rapamycin-Eluting Stent Evaluated At Rotterdam Cardiology Hospital (RESEARCH) and Taxus-Stent Evaluated At Rotterdam Cardiology Hospital (T-SEARCH) registries. *J Am Coll Cardiol*. 2006; 47:1530–1537.
2. Kim YH, Dangas GD, Solinas E, Aoki J, Parise H, Kimura M, Franklin-Bond T, Dasgupta NK, Kirtane AJ, Moussa I, Lansky AJ, Collins M, Stone GW, Leon MB, Moses JW, Mehran R. Effectiveness of drug-eluting stent implantation for patients with unprotected left main coronary artery stenosis. *Am J Cardiol*. 2008;101:801–806.

3. Kandzari DE, Colombo A, Park SJ, Tommaso CL, Ellis SG, Guzman LA, Teirstein PS, Tamburino C, Ormiston J, Stone GW, Dangas GD, Popma JJ, Bass TA; American College of Cardiology Interventional Scientific Council. Revascularization for unprotected left main disease: evolution of the evidence basis to redefine treatment standards. *J Am Coll Cardiol*. 2009;54:1576–1588.
4. Gil RJ, Vassilev D, Formuszewicz R, Rusicka-Piekarz T, Doganov A. The carina angle-new geometrical parameter associated with periprocedural side branch compromise and the long-term results in coronary bifurcation lesions with main vessel stenting only. *J Interv Cardiol*. 2009;22:E1–E10.
5. Shimada Y, Courtney BK, Nakamura M, Hongo Y, Sonoda S, Hassan AH, Yock PG, Honda Y, Fitzgerald PJ. Intravascular ultrasonic analysis of atherosclerotic vessel remodeling and plaque distribution of stenotic left anterior descending coronary arterial bifurcation lesions upstream and downstream of the side branch. *Am J Cardiol*. 2006;98:193–196.
6. Vassilev D, Gil R. Clinical verification of a theory for predicting side branch stenosis after main vessel stenting in coronary bifurcation lesions. *J Interv Cardiol*. 2008;21:493–503.
7. Koo BK, Waseda K, Kang HJ, Kim HS, Nam CW, Hur SH, Kim JS, Choi D, Jang Y, Hahn JY, Gwon HC, Yoon MH, Tahk SJ, Chung WY, Cho YS, Choi DJ, Hasegawa T, Kataoka T, Oh SJ, Honda Y, Fitzgerald PJ, Fearon WF. Anatomic and functional evaluation of bifurcation lesions undergoing percutaneous coronary intervention. *Circ Cardiovasc Interv*. 2010;3:113–119.
8. Ryan TJ, Faxon DP, Gunnar RM, Kennedy JW, King SB III, Loop FD, Peterson KL, Reeves TJ, Williams DO, Winters WL Jr. Guidelines for percutaneous transluminal coronary angioplasty. A report of the American College of Cardiology/American Heart Association Task Force on Assessment of Diagnostic and Therapeutic Cardiovascular Procedures (Subcommittee on Percutaneous Transluminal Coronary Angioplasty). *Circulation*. 1988;78:486–502.
9. Popma JJ, Leon MB, Moses JW, Holmes DR Jr, Cox N, Fitzpatrick M, Douglas J, Lambert C, Mooney M, Yakubov S, Kuntz RE; SIRIUS Investigators. Quantitative assessment of angiographic restenosis after sirolimus-eluting stent implantation in native coronary arteries. *Circulation.* 2004;110:3773–3780.
10. Ellis SG, Popma JJ, Lasala JM, Koglin JJ, Cox DA, Hermiller J, O'shaughnessy C, Mann JT, Turco M, Caputo R, Bergin P, Greenberg J, Stone GW. Relationship between angiographic late loss and target lesion revascularization after coronary stent implantation: analysis from the TAXUS-IV trial. *J Am Coll Cardiol*. 2005;45:1193–1200.
11. Medina A, Suárez de Lezo J, Pan M. A new classification of coronary bifurcation lesions. *Rev Esp Cardiol*. 2006;59:183.
12. Ramcharitar S, Onuma Y, Aben JP, Consten C, Weijers B, Morel MA, Serruys PW. A novel dedicated quantitative coronary analysis methodology for bifurcation lesions. *EuroIntervention*. 2008;3:553–557.
13. Girasis C, Serruys PW, Onuma Y, Colombo A, Holmes DR Jr, Feldman TE, Bass EJ, Leadley K, Dawkins KD, Morice MC. 3-Dimensional bifurcation angle analysis in patients with left main disease: a substudy of the SYNTAX trial (SYNergy Between Percutaneous Coronary Intervention with TAXus and Cardiac Surgery). *J Am Coll Cardiol Cardiovasc Interv*. 2010;3:41–48.
14. Louvard Y, Thomas M, Dzavik V, Hildick-Smith D, Galassi AR, Pan M, Burzotta F, Zelizko M, Dudek D, Ludman P, Sheiban I, Lassen JF, Darremont O, Kastrati A, Ludwig J, Iakovou I, Brunel P, Lansky A, Meerkin D, Legrand V, Medina A, Lefèvre T. Classification of coronary artery bifurcation lesions and treatments: time for a consensus! *Catheter Cardiovasc Interv.* 2008;71:175–183.
15. Rodriguez-Granillo GA, García-García HM, Wentzel J, Valgimigli M, Tsuchida K, van der Giessen W, de Jaegere P, Regar E, de Feyter PJ, Serruys PW. Plaque composition and its relationship with acknowledged shear stress patterns in coronary arteries. *J Am Coll Cardiol*. 2006;47:884–885.
16. Kang SJ, Mintz GS, Kim WJ, Lee JY, Park DW, Yun SC, Lee SW, Kim YH, Lee CW, Han KH, Kim JJ, Park SW, Park SJ. Effect of intravascular ultrasound findings on the long-term repeat revascularization in patients undergoing drug eluting stent implantation for severe unprotected left main bifurcation narrowing. *Am J Cardiol*. 2010;107:367–373.
17. Oviedo C, Maehara A, Mintz GS, Tsujita K, Kubo T, Doi H, Castellanos C, Lansky AJ, Mehran R, Dangas G, Leon MB, Stone GW, Templin B, Araki H, Ochiai M, Moses JW. Is accurate intravascular ultrasound evaluation of the left circumflex ostium from a left anterior descending to left main pullback possible? *Am J Cardiol*. 2010;105:948–954.

CLINICAL PERSPECTIVE

To assess geometric changes responsible for acute lumen loss at the left circumflex coronary artery (LCX) ostium after crossover stenting from the left anterior descending coronary artery (LAD) to the left main artery, 23 left main bifurcation lesions with a preprocedural angiographic stenosis of $<50\%$ at the LCX ostium were evaluated by intravascular ultrasound. Using both prestenting and poststenting pullbacks, changes in minimal lumen area (MLA) within the LCX ostium (ΔL), external elastic membrane (EEM) area at the MLA site (ΔV), and plaque+media area at the MLA site (ΔP) were calculated. The MLA within the LCX ostium significantly decreased from 5.4 mm^2 prestenting to 4.0 mm^2 poststenting ($P<0.001$). The percent change in MLA within the LCX ostium correlated with changes in EEM eccentricity at the LCX carina ($r=-0.414$, $P=0.049$) and percent change in EEM area at the MLA site ($r=0.626$, $P=0.001$). A smaller distal carina angle between the LAD and the LCX prestenting was associated with a greater percent reduction in lumen ($r=0.472$, $P=0.023$) and EEM ($r=0.402$, $P=0.048$) poststenting. In 18 lesions with $>10\%$ reduction of MLA within the LCX ostium, ΔP closely correlated with the ratio of ΔV to ΔL ($r=-0.953$, $P<0.001$), suggesting that an increase in plaque at the LCX ostium contributed to MLA loss relative to the decrease in EEM area. Lumen loss at the LCX ostium frequently occurred after crossover stenting from the distal left main artery to the LAD. The main mechanism was carina shift associated with a narrow angle between the LAD and the LCX.